Features of low-temperature tunneling magnetoresistance of pressed chromium dioxide CrO_2 nanopowders

Yu. A. Kolesnichenko, N. V. Dalakova, E. Yu. Beliayev, O. M. Bludov, and V. A. HorielyiO. M. Osmolowskaya and M. G. Osmolowsky

Citation: Low Temperature Physics **43**, 617 (2017); doi: 10.1063/1.4985216
View online: http://dx.doi.org/10.1063/1.4985216
View Table of Contents: http://aip.scitation.org/toc/ltp/43/5
Published by the American Institute of Physics

Features of low-temperature tunneling magnetoresistance of pressed chromium dioxide CrO_2 nanopowders

Yu. A. Kolesnichenko, N. V. Dalakova,[a] E. Yu. Beliayev, O. M. Bludov, and V. A. Horielyi

B. Verkin Physics and Technology Institute for Low Temperatures, NAS Ukraine, 47 Nauka Ave., Kharkov 61103, Ukraine

O. M. Osmolowskaya and M. G. Osmolowsky

St. Petersburg State University, Chemistry Faculty, St. Petersburg 198504, Russia

(Submitted August 16, 2016)
Fiz. Nizk. Temp. **43**, 772–781 (May 2017)

A study of the resistive and low-temperature magnetoresistive properties of pressed powders of ferromagnetic half-metal chromium dioxide CrO_2 with nanoparticle shape anisotropy. The effects of Fe impurities on the tunneling resistance and magnetoresistance of CrO_2 powders are investigated. It is found that the Fe impurity leads to a decrease in the resistance and tunneling magnetoresistance of chromium dioxide. It is suggested that the decrease in magnetoresistance of the solid solution $Cr_{1-x}Fe_xO_2$ is associated with the formation of additional localized states at the iron impurities in a tunnel barrier. The influence of the magnetic field input rate on the form of the low-temperature tunneling magnetoresistance hysteresis in $Cr_{1-x}Fe_xO_2$ powder is considered. It is shown that the low-temperature singularities of magnetoresistance hysteresis depend on the relaxation rate of the magnetic moments of the nanoparticles to the equilibrium state. Possible reasons for such a dependence are discussed. *Published by AIP Publishing.* [http://dx.doi.org/10.1063/1.4985216]

Introduction

Chromium dioxide (CrO_2) is one of the most famous and widely used magnetic materials. This is the only oxide ferromagnet that exists at room temperature. In fine-particle form CrO_2 has long been used for devices that read and record information. At present, as a ferromagnetic half-metal with a Curie temperature of $T_C \approx 390$ K (Refs. 1 and 2) CrO_2 may be of interest in the study of spin-polarized transport and usage in spintronic devices. It is known that the efficiency of spintronic devices depends on the maximum attainable magnetoresistance (MR). In this regard, the prospects of using chromium dioxide powder are tied to the development of technology for obtaining powders with a high MR. Regardless of the fact that the intrinsic MR of single crystal CrO_2 at room temperature is about 1% in a field $H = 1$ T[3] and varies slightly with decreasing temperature, the MR turns out to be gigantic in a composite granular material consisting of CrO_2 particles coated with a thin dielectric layer. The MR of granular material can be more than 30% at low temperatures and low fields.[2,4] Such a MR is extrinsic. It is caused by the intergranular spin-dependent tunneling and depends on the properties of magnetic tunnel junctions between ferromagnetic granules and on the relative orientation of the magnetization vector in neighboring granules. This type of MR is called tunneling magnetoresistance. Earlier in Refs. 5–7, we considered the impact that various factors controlled by synthesis technology have on the magnitude of tunneling MR. Such factors include the thickness and type of dielectric interlayers between CrO_2 particles, as well as the nanoparticle shape anisotropy. The maximum value of the negative tunneling MR (about 36% at temperatures of $T \leq 5$ K in fields up to 0.3 T) was obtained for powders consisting of needle-like particles with a thickness of dielectric coating $\sim$2 nm. The purpose of this study is to investigate the effect of a ferromagnetic metal impurity on the resistance and magnitude of the MR of chromium dioxide powders, as well as to study the low-temperature hysteresis behavior of tunneling MR of CrO_2 samples with iron impurities.

One of the most intriguing and insufficiently studied features of low-temperature MR behavior of CrO_2 powders is their non-monotonic dependence of the MR on the magnetic field. It is found that as the magnetic field increases the absolute value of the MR first increases rather rapidly, and then starts to decrease noticeably, forming a maximum.[6] Such behavior of MR at low temperatures ($T \leq 10$ K) was observed for all CrO_2 samples with particle shape anisotropy. For samples consisting of spherical CrO_2 particles, non-monotonic dependence was either negligibly manifested, or not at all. The non-monotonic dependence for MR contradicts the usually observed MR hysteresis for transition metal magnetic oxides. For such materials, an increase in the field is usually accompanied by a monotonic increase of negative MR: a sharp increase in low fields followed by a slower growth as the magnetization of the sample tends to saturation.

A possible cause of the discrepancy between the hysteresis of magnetization and MR of inhomogeneous granular magnetic systems is the percolative nature of conductivity. At low temperatures the conductivity is determined by a small volume fraction of the granules, and local magnetic properties of this part of the granules can differ from the universal magnetization of the bulk sample, measured by the magnetometer. Despite the fact that the effect the granularity has on the observed anomaly in the behavior of MR hysteresis is undoubted, the mechanism responsible for the decrease in the MR of a limited number of conducting channels given a sufficient increase in the field, remains unclear.

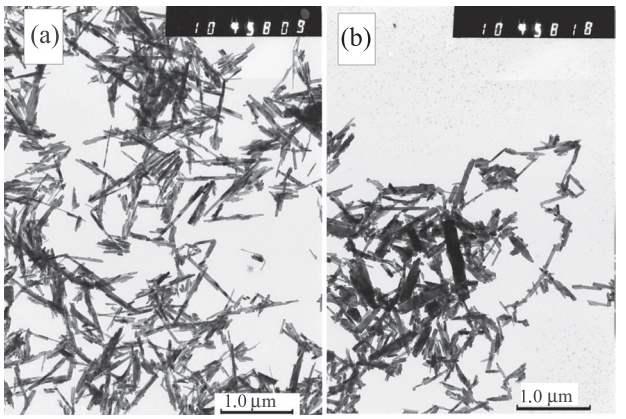

Fig. 1. Micrographs of the two powders, obtained using a transmission electron microscope: powder No. 1 (CrO_2) (a); powder No. 2 ($Cr_{1-x}Fe_xO_2$)(b).

Methods of preparation and investigation of the samples

This paper presents the results of measuring the temperature dependences of resistance in a broad range of temperatures (4.2–300 K) as well as the results of studying the low-temperature magnetoresistive properties of two pressed chromium dioxide powders. One such sample (sample no. 1) is a pure CrO_2 powder, whereas the second (sample no. 2) is a solid solution of CrO_2-Fe. The iron content in sample no. 2 was 75 mmol/(1 mol chromium). Both powders were prepared under the same conditions and consisted of needle-shaped particles with a diameter-to-length ratio of 1:10.

The powders were prepared by hydrothermal synthesis. General features of the used synthesis technology are described in Ref. 8. CrO_2 particles were coated with a dielectric shell, which was a natural degraded layer consisting of a mixture of amorphous β-CrOOH and some occluded chromic acid.

In Ref. 9 Mössbauer spectroscopy is used on ^{57}Fe atoms to establish that Fe^{3+} ions in chromium dioxide powders are distributed between three magnetic solid solutions. In addition to solid solutions $Cr_{1-x}Fe_xO_2$ (this is a massive substance and an iron-enriched surface layer) and including $Cr_{2-2x}Fe_{2x}O_3$ particles, the iron is present in the chromium oxyhydroxide β-CrOOH, which is part of the dialectic shell. Thus we believe that in sample no. 2 the iron is present in two forms: as a $Cr_{1-x}Fe_xO_2$ solid solution and as $Cr_{2-2x}Fe_{2x}O_3$. The first compound ensures the high coercive force. The second phase is a ballast and is present as separate small particles. These particles are antiferromagnetic or their magnetization is two orders of magnitude lower than that of CrO_2. The $Cr_{2-2x}Fe_xO_3$ phase is dielectric and does not contribute to the conductivity. The concentration of iron varies across the thickness of the particle. On the surface it is much higher, and therefore the magnetization reversal is controlled by the composition of the surface.

TABLE 2. Magnetic characteristics of two samples at 4.2 K. Maximum magnetization M_{max} was estimated in a field of 5 T.

			M, A m^2/kg			
Sample No.	H, Oe	H_p, Oe	M_{max}	M_{res}	H_A, Oe	H'_A, Oe
1	848	232	101.10	31.93	3804	>1500
2	1138	376	76.25	28.03	4592	6975

The finished powders were tested by electron microscope, x-ray, and magnetic methods. Micrograph examples of the two test powders, obtained using the JEOLS JEM-107 transmission electron microscope are shown in Fig. 1. Cold pressing of the samples was used to form tablets in the shape of parallelepipeds having the dimensions 3 × 5 × 12 mm.

The magnetic properties of the samples were measured on a vibrational (77 Hz) and SQUID (Quantum Design) magnetometer. The temperature dependence of the resistivity was taken using the four-probe method in a set current mode $J = 100$ μA with fulfillment of Ohm's law. For resistive measurements the distance between the potential contacts was 8 mm. The Keithley-2182 nanovoltmeter and the Keithley-2000 multimeters were used to record the voltage and current. The MR as a function of the magnetic field, written as $\Delta R(H)/R(0) = [R(H) - R(0)]/R(0)$ was written according to the usual protocol of writing hysteresis cycles of magnetization in sequence $+H_{max} \rightarrow 0 \rightarrow -H_{max} \rightarrow 0 \rightarrow +H_{max} \rightarrow 0$. The magnetic field interval was ±1.5 T while MR was recorded. The MR measurements were performed using a rotating Kapitsa magnet.

The main characteristics of the test powders are given in Tables 1 and 2. The data presented in the tables show that the Fe impurity changes not only all the magnetic characteristics of the powder, but that it also affects the parameters of the CrO_2 lattice.

Results and discussion

The results of measuring the magnetic characteristics of two powders are shown in Figs. 2–4. The temperature dependences of the specific magnetization $M(T)$ recorded in the ZFC (zero field cooling) and FC (field cooling) modes show that the introduction of an iron impurity with the formation of a solid substitutional solution $Cr_{1-x}Fe_xO_2$ leads to a decrease in magnetization of the pure CrO_2 powder and an increase in the Curie temperature (see Fig. 2 and Table 1). In order to determine the Curie temperature we used the FC

TABLE 1. Change in the main parameters of CrO_2 powder upon the introduction of Fe impurity.

			M, A m^2/kg							
Sample No.	T_C, K	H_c, Oe	M_{max}	M_{res}	$k_п$	a, Å	c, Å	V_{cell}, Å^3	$S_{specific}$, m^2/g	d_{eff}, nm
1	398 ± 1	522	83.9	36.6	0.437	4.4253	2.9120	57.0265	34	24
2	414 ± 5	761	75.3	34.6	0.459	4.4270	2.9140	57.1095	24	34

Note: H_c is the coercive force, M_{max},M_{res} are the maximum and residual magnetization of the samples, respectively, $k_п$ is the rectangularity of the hysteresis loop, a and c are the rutile lattice parameters, $S_{specific}$ is the specific surface area, d_{eff} is the effective particle diameter, V_{cell} is the unit cell volume. The magnetic characteristics correspond to a temperature of 293 K.

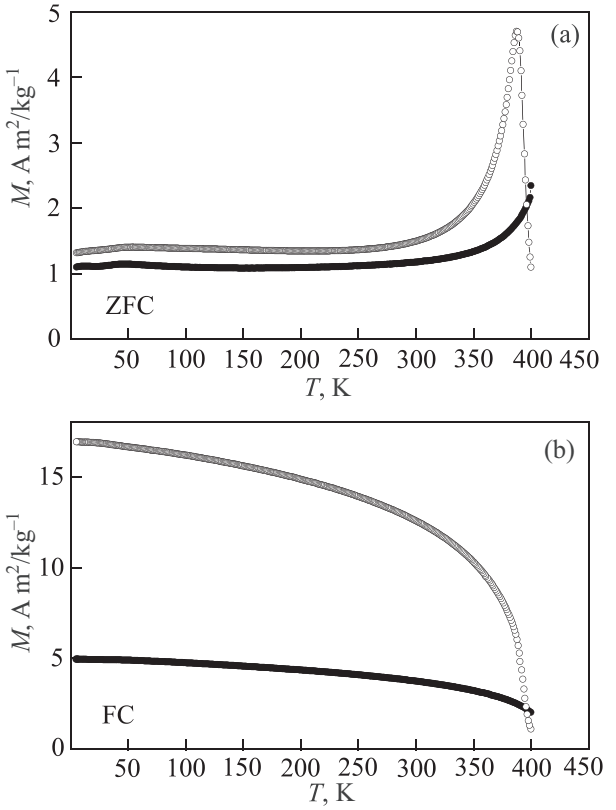

Fig. 2. The magnetization of sample no. 1 (○) and no. 2 (●) as a function of temperature, recorded in a field of 100 Oe in FC and ZFC regimes.

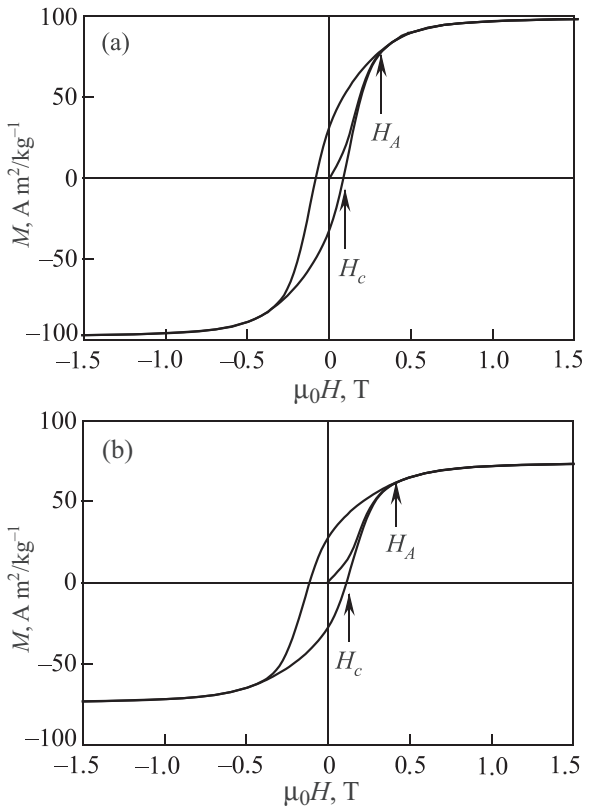

Fig. 3. The hysteresis loops of magnetization for sample no. 1 (a) and no. 2 (b), recorded at a temperature of 4.2 K. The arrows indicate the anisotropy fields H_A of the macroscopic samples, and the coercive force H_c.

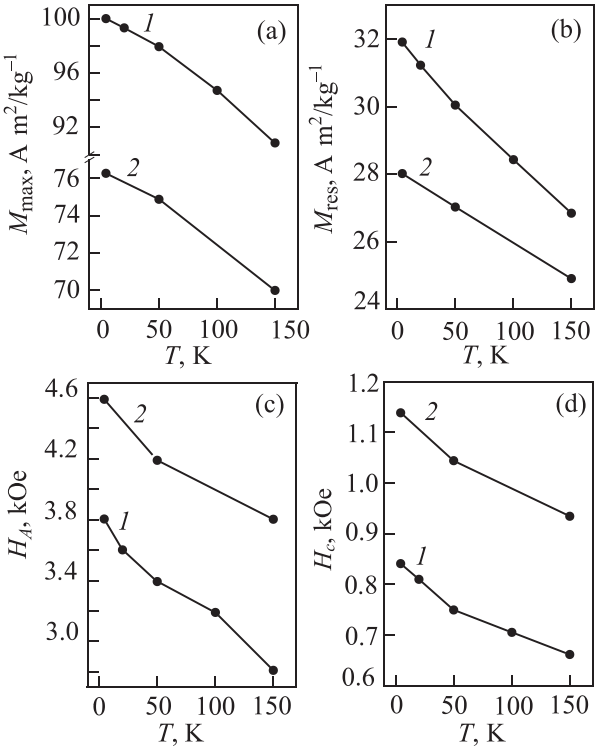

Fig. 4. The temperature dependences of the maximum magnetization (a), residual magnetization (b), anisotropy fields (c) and coercive force (d). The numbers of the curves correspond to the Sample numbering. The maximum magnetization was determined in a field of 5 T.

dependences $M(T)$. For Sample No. 1 the high-temperature region of the $M(T)$ dependence near the magnetic ordering temperature wherein the magnetization decreases sharply, was approximated by a linear function. The Curie temperature is determined from the point of intersection of this function with the abscissa axis (398 ± 1 K). For sample no. 2 the Curie temperature turned out to be greater than the maximum temperature in the experiment of $T = 400$ K. Taking into account the comparatively low iron content and the qualitative similarity of the functional dependence $M_{FC}(T)$ of the two samples, we assumed that these dependences should coincide in the relative coordinates $y = M(T)/M(5\,\text{K})$, $x = T/T_C$, wherein T_C is the Curie temperature of the corresponding sample. Using the above assumption and the value of the Curie temperature for sample no. 1 it is possible to determine the Curie temperature of sample no. 2. Regardless of the fact that it is a fairly crude approach that has its share of flaws, it gave a reasonable value of $T_C = 414 \pm 5$ K for a sample with an iron impurity (no. 2).

Comparing the temperature dependences of magnetization in ZFC and FC regimes for each of the samples reveals a fairly large difference between the $M_{ZFC}(T)$ and $M_{FC}(T)$ curves, even at temperatures close to T_C. It follows from this fact that at $H = 100$ Oe the directions of the magnetic moments of the particles in CrO_2 and $Cr_{1-x}Fe_xO_2$ powders are blocked by anisotropy fields, and in low fields the magnetization is in disequilibrium at all temperatures $T \leq T_C$. This means that at $T \leq T_C$ there is irreversible magnetization reversal.

Low-temperature measurements of magnetization hysteresis were performed at several temperatures over the interval of 4.2–150 K. As an example Fig. 3 shows hysteresis

loops $M(H)$ of two samples, recorded at $T = 4.2$ K. A comparison of Figs. 3(a) and 3(b) reveals that the iron impurity noticeably decreases the maximum and residual magnetization of the powder CrO_2, increasing the coercive force H_c and anisotropy field H_A (see Table 2). The same changes to the magnetic parameters are found throughout the entire temperature range of the measurements with the introduction of the iron impurity (see Fig. 4). The monotonic change with the temperature of residual magnetization and anisotropy field in Fig. 4 serves as evidence of the fact that even at $T \approx 4.2$ K a part of the particles in powders No. 1 and No. 2 remains unblocked. The amount of unblocked particles in both samples decreases gradually as the temperature drops. A noticeable decrease in the maximum magnetization upon addition of the Fe impurity can be partially attributed to the dilution of the ferromagnetic phase $Cr_{1-x}Fe_xO_2$ by the antiferromagnetic phase $Cr_{2-2x}Fe_{2x}O_3$. An antiparallel orientation of the Fe and Cr ions in the main phase of $Cr_{2-2x}Fe_{2x}O_3$ is also possible. As shown in Ref. 9, in addition to the nanoparticle size factor, the concentration of iron impurity in the CrO_2 surface layer is also a regulator of the coercive force. It is established in Ref. 9 that the coercive force of the CrO_2 powder increases almost linearly with increasing iron content. The increase in the anisotropy field and coercive force of the $Cr_{1-x}Fe_xO_2$ powder in comparison to the corresponding values for CrO_2 indicate that the magnetization reversal energy of CrO_2 powder increases substantially with the introduction of the iron impurity.

Since the probability of electron tunneling depends on the direction of the magnetic moments of the neighboring granules, it can be expected that changes to the magnetic behavior of the powder will lead to corresponding changes in the behavior of MR hysteresis. The magnetoresistive measurements of $Cr_{1-x}Fe_xO_2$ were conducted in order to obtain new information about the features of low-temperature tunneling MR of pressed CrO_2 powders. At the same time, as noted above, under the conditions of activated conductivity the low-temperature MR of the granular system depends on the magnetic properties of a limited number of conducting channels, such that the magnetization reversal conditions of that part of the granules that participates in the conductivity may differ from the magnetization reversal of the bulk of the sample.

Let us consider the results of resistive and magnetoresistive studies. Measurements of the temperature dependence of resistivity were performed over the 4.2–300 K interval. Figure 5 demonstrates the nonmetallic behavior of the resistance ($d\rho/dT < 0$) of two samples. At $T < 20$ K the dependence of $\rho(T)$ is almost exponential, which points to the tunneling nature of conductivity. For a solid solution $Cr_{1-x}Fe_xO_2$ (sample no. 2) lower values of resistivity were obtained. At the same time the negative MR of this sample turned out to be lower than the MR of sample no. 1 (Fig. 6). Since the type, quality, and thickness of the dielectric coating of the particles in the two powders are about the same, it can be assumed that the observed changes to the resistance values of sample no. 2 in zero (Fig. 5) and finite magnetic field (Fig. 6) are mainly related to the presence of iron impurities. The results of measuring $\rho(T)$ and tunneling MR are shown in Figs. 5 and 6, and demonstrate that the influence of the impurity on the conductivity of the tunneling system is ambiguous. Impurities that are present in the dielectric layer can facilitate the simple tunneling of electrons, decreasing

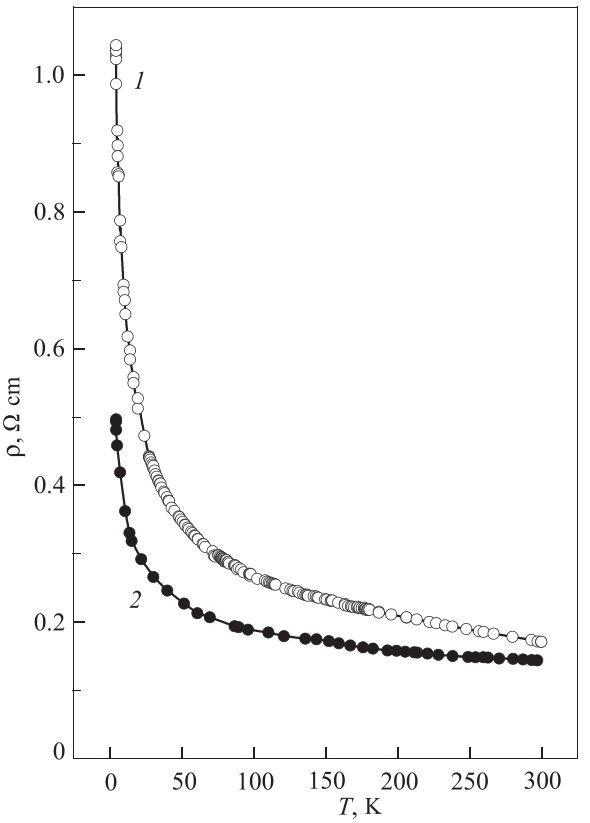

Fig. 5. The temperature dependences of resistivity for sample no. 1 (○) and sample no. 2 (●). The current $J = 100$ μA.

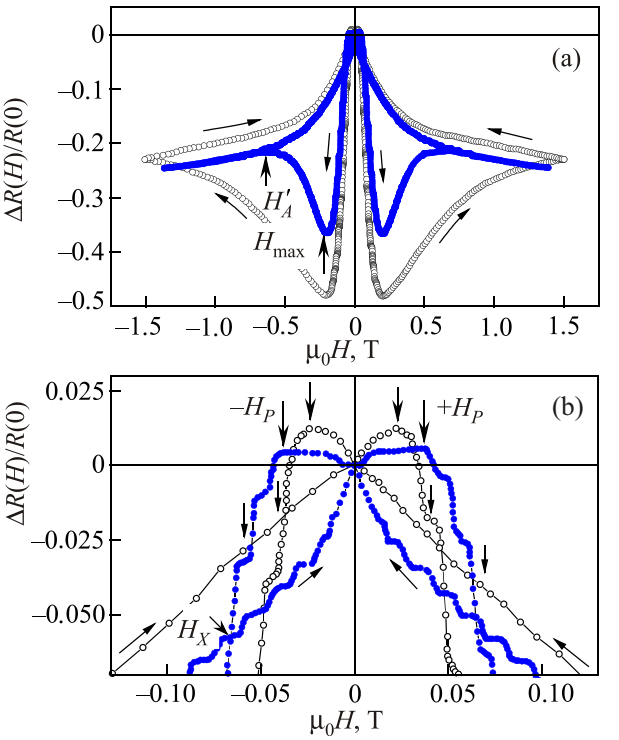

Fig. 6. (a) MR hysteresis curves, taken at a temperature of $T = 4.25$ K in a magnetic field $\mathbf{H}||\mathbf{J}$ ($dH/dt \cong 0.021$ T/s). (○) is sample no. 1. (●) is sample no. 2. Panel (b) shows the corresponding MR dependences on an enlarged scale in the range of low fields. H_p is the field of the positive MR maximum, H_X is the intersection field of the field input and output curves.

the resistance of the system (Fig. 5). On the other hand, these same impurities hamper the magnetic (depending on spin) tunneling, which leads to a decrease in MR (see Fig. 6). These changes occur due to the formation of additional localized states in the tunnel barriers. Localized states can be formed both on Fe ions that are present in the surface dielectric layer of the nanoparticles, and on $Cr_{2-2x}Fe_{2x}O_3$ impurities that are located in the intergranular dielectric medium as separate small particles.[9] A decrease in the MR of solid solutions $Cr_{1-x}Fe_xO_2$ can be explained by two reasons: by a decrease in magnetization of some of the ferromagnetic granules and the loss of the electron spin orientation during tunneling through a chain of electron states localized at the tunnel barrier due to processes occurring with a spin flip. The last mechanism for decreasing the MR is considered in Ref. 10 for the case of tunnel ferromagnet-insulator-ferromagnet junctions involving a half-metal. Additional contributions to the decrease in spin polarization can also result from a random impurity distribution.

In Fig. 6, the MR curves in the low-field region reveal a small positive MR, with a maximum $\pm H_p$ that has to correspond to the coercive force H_c. As we can see, introducing the Fe impurity leads to a marked increase in the coercivity field H_p, found from resistive measurements, which correlates to the results of the magnetic measurements.

In granulated half-metals tunneling conductivity is defined by two factors: the thickness and properties of the intergranular dielectric layers and the orientation of the magnetic moments of the neighboring granules. For this reason the behavior of the hysteresis curves of tunneling MR must reflect the well-known hysteresis behavior of magnetization $M(H)$: a sharp increase in $M(H)$ with a field increase in the range of low fields with subsequent weak growth to saturation. In our case the behavior of the MR hysteresis curves shows the absence of a correlation between the behavior $M(H)$ and $\Delta R(H)$. In some low field $H_X > H_p$ we observe an additional intersection of field input and output curves [see Fig. 6(b)]. This leads to the appearance of a second hysteresis $\Delta R(H)$. For this hysteresis the field output curves at $H > H_X$ are located lower than the input curves, which corresponds to a lower value of magnetization for the sample at field output. Such MR behavior does not coincide with the magnetization behavior, since the $M(H)$ dependences have only one hysteresis in the fields $H < H_A$ (see Fig. 3). The MR hysteresis described above was observed by us even earlier.[5–7,11] It is related to the percolative nature of tunneling conductivity of the granular system at low temperatures and is explained by the switching of the limited number of current channels during the interchanges of the magnetic field.

The second anomalous feature of low-temperature negative MR behavior is shown on Fig. 6 and is the decrease in $\Delta R(H)$ with an increase in magnetic field, starting from relatively low fields of $H_{\max} \cong 0{,}2$ T, wherein $H_{\max}$ is the field of the negative MR maximum. This effect decreases and gradually disappears with increasing temperature or measuring current (Fig. 7).

For a solid $Cr_{1-x}Fe_xO_2$ solution there is a new feature along the behavior of $\Delta R(H)$. Starting from some field H'_A that is equal to the coupling field of the ascending and descending branches of the $\Delta R(H)$ dependence [Fig. 6(a)], the decrease in the negative MR with an increasing field is

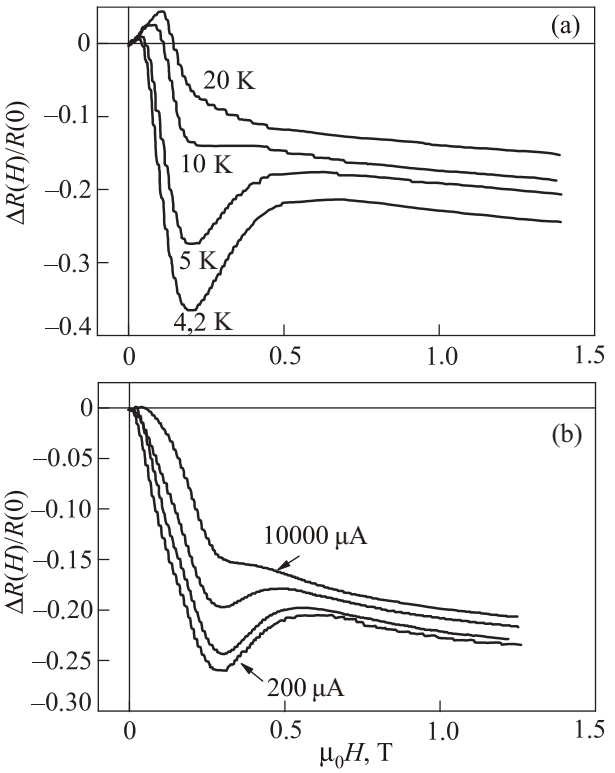

Fig. 7. (a) The dependences $\Delta R(H)/R(0)$ for sample no. 2, recorded at various temperatures ($J = 100$ μA, **H**||**J**). (b) The dependences $\Delta R(H)/R(0)$ for sample no. 2 recorded at various currents, μA: 200, 2000, 5000, 10 000 ($T = 4.93$ K, **H**||**J**). The field input rate $dH/dt = 0.021$ T/s.

replaced by its repeat growth. By analogy to the behavior of the $M(H)$ hysteresis we will conditionally label the field H'_A as the anisotropy field. This field does not correspond to the anisotropy field H_A found from the magnetic measurements. The field H_A blocks the directions of the magnetic moments of the particles during demagnetization of the bulk sample by an external field. Field H'_A "blocks" the direction of the magnetic moments of separate particles and nanoclusters that form the conductive channels in the "dielectric" matrix at low temperatures. The formation of nanoclusters can be associated with local inhomogeneity in the thickness of the dielectric particle shells: the value H'_A is determined by the ratio of the external field energy, the magnetic anisotropy energy, and the dipole-dipole interaction energy between the nanoparticles and nanoclusters. In any case in fields $H < H'_A$ the system exists in a blocked state. The blocking condition is $\tau > t_i$, wherein τ is the relaxation time of the particle magnetic moments to an equilibrium distribution in orientations, and t_i is the observation time. When $\tau < t_i$ the system is able to reach an equilibrium state during the observation time and the hysteretic behavior of MR is not manifested. The ratio between τ and t_i, can be changed either by increasing the temperature (decreasing τ) or increasing the observation time t_i. The second approach can be implemented by decreasing the rate of magnetic field input dH/dt at a fixed temperature. As dH/dt decreases gradually the observation time $t_i \to \tau$. It follows that in fields $H < H'_A$ the type of MR hysteresis must depend on the rate of magnetic field input. In order to test this assumption, we recorded the hysteresis loops $\Delta R(H)$ for sample no. 2 at various magnetic field pulling rates. The results of this experiment are shown in Fig. 8. For further discussion we denote the branches of the

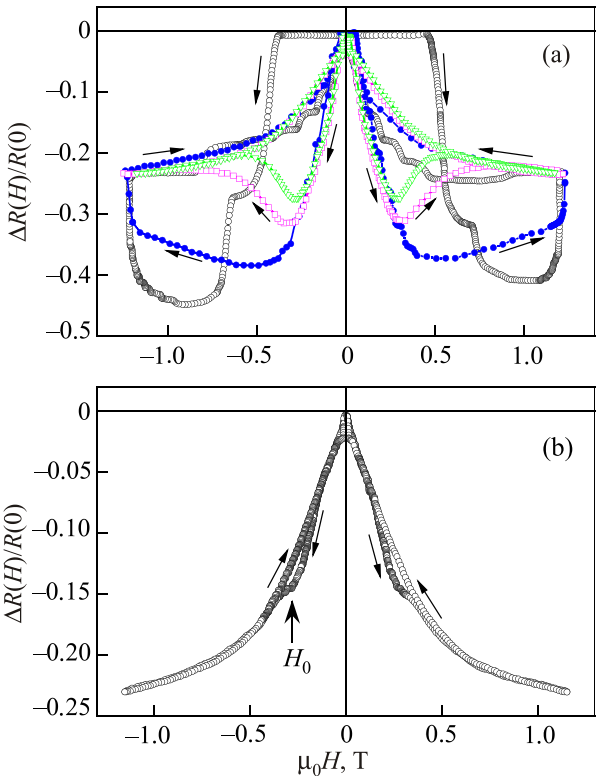

Fig. 8. (a) MR hysteresis curves of sample no. 2 at $T = 4.25$ K, recorded at various magnetic field pulling rates: (○) 0.25 T/s, (●) 0.125 T/s, (□) 0.037 T/s; (▽) 0.021 T/s. (b) The MR hysteresis curves of sample no. 2 at a temperature of $T = 4.25$ K recorded at a minimum magnetic field pulling rate $dH/dt = 0.0029$ T/s. The magnetic field is perpendicular to the plane of the sample and perpendicular to the current. $J = 100$ μA.

hysteresis curves corresponding to the input of the magnetic field as $\Delta R(H^{\uparrow})$, and branches corresponding to field output as $\Delta R(H^{\downarrow})$.

The experimental data on Fig. 8 show that the shape of the MR hysteresis loops are definitely defined by the rate of the magnetic field input $dH^{\uparrow}/dt$. At the same time the field output curves $\Delta R(H^{\downarrow})$ are practically the same for all values $dH^{\downarrow}/dt$. As $dH^{\uparrow}/dt$ decreases, so does the area of the hysteresis loop, the coercive field H_p, the value $\Delta R(H^{\uparrow}_{\max})$, and the field of the negative MR maximum $(H^{\uparrow}_{\max})$. Given a minimum magnetic field input rate $dH^{\uparrow}/dt$=0.0029 T/s the curves $\Delta R(H^{\uparrow})$ and $\Delta R(H^{\downarrow})$ practically collapse, and the extremum on the field input curve degenerates into a small shoulder at H_0 [Fig. 8(b)]. As such, the magnetic field input curves $\Delta R(H^{\uparrow})$ correspond to the non-equilibrium state of the magnetic system ($\tau > t_i$). As $dH^{\uparrow}/dt$ decreases the observation time increases ($t_i \to \tau$) and the magnetic system gradually approaches the equilibrium state ($\tau < t_i$).

Given a fixed value of $dH^{\uparrow}/dt$ the value $\Delta R(H^{\uparrow}_{\max})$ can depend only on the rate of relaxation of the magnetic spin subsystem to the equilibrium state. The relaxation time τ is determined by the competition between the action of the external field H and the total action of the internal demagnetizing fields. Figure 8(b) shows that even at a minimum rate $dH/dt = 0.0029$ T/s the equilibrium state of the magnetic system is not yet reached. This is confirmed by data from Fig. 9, which shows the time scan of $\Delta R(H_i,t)$ recorded at various fixed fields H_i. The protocol for recording the MR was as follows. After magnetization reversal of the sample the magnetic field was gradually input over the course of

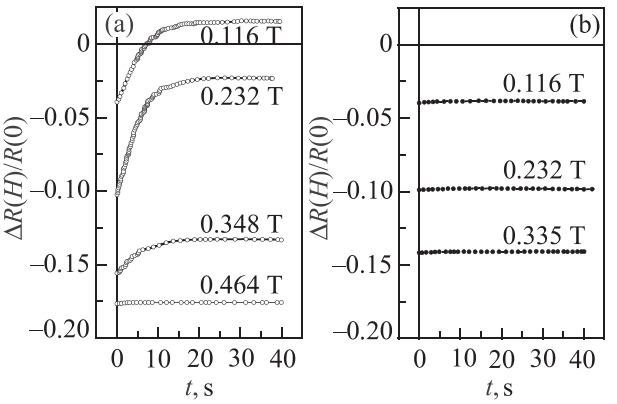

Fig. 9. Time scan of negative MR of sample no. 2 in different fields **H**⊥**J** when adding (a) and removing (b) a magnetic field. The field input rate $dH/dt = 0.0029$ T/s, $J = 100$ μA, $T = 4.25$ K.

40 s at a minimum rate equal to 0.0029 T/s, until reaching a value of 0.116 T. Afterward the field was stabilized and the time dependence $\Delta R(t)$ was recorded at $H = 0.116$ T. This procedure was repeated with increases in the magnetic field in intervals of $\Delta H = 0.116$ T until a state close to the equilibrium was reached at $H = 0.464$ T. In this state a decrease in $\Delta R(H,t)$ was almost absent [see Fig. 9(a)]. The time scan of magnetic field output curves was similarly recorded [Fig. 9(b)].

Figure 9 shows that the rate of MR decrease with time $(d\Delta R(H)/dt)$ decreases gradually during magnetic field input as the field tends to the anisotropy field value $H'_A \cong 0,47$ T. Magnetic field input curves at $H < H'_A$ correspond to the non-equilibrium state of the system. As such, the results of the time scan confirm that in addition to the external magnetic field the spin system is also affected by the demagnetizing factor, which stands in the way of magnetizing the sample as the field is introduced, and tries to return the system to its equilibrium state when the field input is stopped.

The relaxation processes during magnetization and magnetization reversal can be associated with both the action of the anisotropy fields and the dipole-dipole interaction between the needle-like nanoparticles and clusters that form the transport channels. The magnetic anisotropy can have various attributes. However the main factor that forms the magnetic anisotropy of the sample is the anisotropy of the particle shape. In needle-like particles that have a diameter of 24–34 nm and a length of ~300 nm there is uniaxial magnetic anisotropy, since the c axis of the easy magnetization of CrO_2 is practically the same as the symmetry axis of the particle. During the process of pressing the powder the needle-like particles are deposited mainly into the plane of the sample, though in the plane itself they are randomly distributed. This forms the magnetic texture in which the magnetization in the plane of the sample significantly exceeds the magnetization in the perpendicular direction (see Fig. 2). When the magnetic field is switched off or stabilized a part of the magnetic moments of the particles oriented along the field tends to turn in the direction of the easy magnetization axis. At this moment a mismatch of the magnetic moments of individual FM granules occurs, and tunneling probability decreases. As a result the negative MR decreases as well (see Fig. 9).

The features of $\Delta R(H)$ behavior described above are manifested only at low temperatures, when the conductivity

of the granular structure has a percolative nature and MR is determined by the conductivity of a small number of "optimal" chains of granules with maximum tunneling probability. Under the conditions of activation conductivity the number of "optimal" conductive channels decreases continuously with decreasing temperature, and given a sufficiently low temperature the percolative grid can be reduced to a single conducting channel.[12] The qualitative difference between the MR hysteresis at high ($T > 10$ K) and low ($T < 10$ K) temperatures means that the magnetization reversal processes of the macroscopic ensemble of ferromagnetic granules in quasi-one-dimensional chains of granules (structures with reduced dimensionality) occur according to different scenarios. The "optimal" conducting chains can have several weak links (high-resistance tunnel junctions) and increased activation energy. These highly resistive junctions are what determine the overall conductivity of the system. Given a fixed temperature the spatial position of the "optimal" chains of granules with maximum conductivity (and position of the high-resistance junctions inside these chains) varies continuously with changes to the external magnetic field. Increases in the external magnetic field decrease the potential barriers between the FM granules, thus increasing the permeability of the tunnel barriers. This opens up additional transport channels and leads to an elongation of the conducting chains-clusters with a reduced activation energy of the already-existing transport channels located inside.[13] As a result there is a sharp increase in the negative MR in low fields. However the process of increasing the length of the clusters gradually changes the ratio between the external magnetic field, the anisotropy field, and the dipole-dipole interaction field.[14] At $H = H_{max}$ the demagnetization factor becomes stronger than the action of the external field and MR starts to decrease.

Since there is always some blurring between the energy levels of electron states in the neighboring granules, conduction electrons must acquire a certain energy (from phonons, for instance) in order for tunneling to occur. At low temperatures the number of phonons with the necessary energy is limited, and therefore for a single tunnel junction the number of carriers that come to the junction over a certain period of time Δt can be greater than the number of carries that leave the junction during the same time. As a result when the magnetic field is introduced the process of charge transfer is blocked in sufficiently low fields, which also leads to a decrease in conductivity (decrease in negative MR). As the field input rate is decreased a part of the electrons has time to obtain energy from a phonon and tunnel, however during time $t \leq \tau$ the magnetic system partially relaxes to the equilibrium state. This leads to a decrease in the MR peak at H_{max} and a gradual disappearance of the second hysteresis. This process is accompanied by a general reduction in tunneling MR.

Conclusion

A study of the magnetic, resistive and magnetoresistive properties of two pressed powders consisting of ferromagnetic chromium dioxide particles separated by dielectric layers is conducted. One of these powders was composed of needle-shaped CrO_2 particles, the second was made of $Cr_{1-x}Fe_xO_2$ needle-like particles. It is shown that the Fe impurity has a significant impact on the magnetic properties, resistance and spin-dependent tunneling MR in pressed chromium dioxide nanopowders.

- New results have been obtained, of which the following can be noted.
- The Fe impurity significantly decreases the resistance and tunneling MR of CrO_2 powders. This effect can be explained by the formation of additional localized states on the Fe impurities in the tunnel barrier.
- At low temperatures the pressed powders exist in a blocked state. The MR value and the position of the MR maximum are determined by the rate of relaxation of the magnetic subsystem of the pressed ferromagnetic nanoparticles to the equilibrium state and depend on the rate of the magnetic field input.
- Low-temperature features of tunneling MR indicate that the magnetic behavior of a limited number of transport channels consisting of a sequence of ferromagnetic granules and clusters differs from the magnetic properties of the bulk sample.

As such, the general features of low-temperature behavior of tunneling MR of pressed CrO_2 powders can be explained by the granular structure and the formation of a magnetic texture. At the same time, based on our results we cannot make an unambiguous conclusion as to the mechanism responsible for the spin relaxation in the test samples. In addition to the action of uniaxial anisotropy fields, the percolative system of pressed FM half-metal CrO_2 powders is subject to the forces of interparticle dipole-dipole interaction. At low-temperatures as the magnetic field increases there can be a lengthening of the conducting clusters in percolation chains. In this case the interparticle dipole-dipole interactions will be enhanced, and the qualitative scenario of how this system will behave in a magnetic field will become very complex. Therefore, the considered problem requires more detailed investigation.

The results obtained in this study serve as evidence of the possibility of impacting the resistive characteristics of granular systems composed of CrO_2 nanoparticles via controlled changes to the content of ferromagnetic impurities, as well as by changing the nanoparticle shape anisotropy.

The authors wish to express their deepest gratitude to Dr. Sc. (Phys-Math.) A. I. Kopeliovich for the useful discussion and for showing an interest in this work.

[a)]Email: dalakova@ilt.kharkov.ua

[1]R. A. Groot, F. M. Mueller, P. G. van Engen, and K. H. J. Buschow, Phys. Rev. Lett. **50**, 2024 (1983).
[2]J. M. D. Coey and M. Venkatesan, J. Appl. Phys. **91**, 8345 (2002).
[3]M. Ziese, Rep. Prog. Phys. **65**, 143 (2002).
[4]J. M. D. Coey, A. E. Berkowitz, L. I. Balcells, F. F. Putris, and A. Barry, Phys. Rev. Lett. **80**, 3815 (1998).
[5]B. I. Belevtsev, N. V. Dalakova, M. G. Osmolowsky, E. Yu. Beliayev, A. A. Selyutin, and Yu. A. Kolesnichenko, Izvestiya RAN, Fiz. **74**, 1111 (2010) [Bull. Russ. Acad. Sci. Phys. **74**, 1062 (2010)].
[6]N. V. Dalakova, B. I. Belevtsev, E. Yu. Beliayev, A. N. Bludov, V. N. Paschenko, M. G. Osmolowsky, and O. M. Osmolowskaya, FNT **38**, 1422 (2012) [Low Temp. Phys. **38**, 1121 (2012)].

[7]N. V. Dalakova, E. Yu. Beliayev, O. M. Osmolowskaya, M. G. Osmolowsky, and V. A. Gorielyi, Bull. Russ. Acad. Sci. Phys. **79**, 789 (2015).
[8]M. G. Osmolowsky, I. I. Kozhina, L. Yu. Ivanova, and O. L. Baidakova, Zh. Prikl. Khim. **74**, 3 (2001).
[9]S. I. Bondarevsky, V. V. Eremin, V. V. Panchuk, V. G. Semenov, and M. G. Osmolowsky, FTT **68**, 77 (2016).
[10]A. M. Bratkovsky, Phys. Rev. B **56**, 2344 (1997).
[11]B. I. Belevtsev, N. V. Dalakova, M. G. Osmolowsky, E. Yu. Beliayev, and A. A. Selutin, J. Alloys Compd. **479**, 11 (2009).
[12]P. Sheng, Philos. Mag. B **65**, 357 (1992).
[13]S. Ju, T.-Y. Cai, and Z. Y. Li, Appl. Phys. Lett. **87**, 172504 (2005).
[14]S. Sankar, A. E. Berkowitz, and D. J. Smith, Phys. Rev. B **62**, 14273 (2000).

Translated by A. Bronskaya